Zou *et al. BMC Plant Biology* (2025) 25:190
https://doi.org/10.1186/s12870-025-06057-0

BMC Plant Biology

RESEARCH Open Access

Integrated transcriptomic and metabolomic analyses provide insights into defense against *Colletotrichum fructicola* in octoploid strawberries

Xiaohua Zou[1*], Yun Bai[1], Ying Ji[1], Liqing Zhang[1], Qinghua Gao[1] and Xianping Fang[1*]

Abstract

Background The *Colletotrichum fructicola* (*C. fructicola*) is a hemibiotrophic fungus, which causes devastating anthracnose in strawberry. At present, the resistance mechanism to *C. fructicola* remains poorly understood.

Results Here, we used RNA-sequencing and liquid chromatography-mass spectrometry (LC-MS) metabolomics to excavate the molecular mechanism of strawberry resistance to *C. fructicola*. The differentially accumulated metabolites (DAMs) and differentially expressed genes (DEGs) were screened at different stages after *C. fructicola* infection in the susceptible 'Benihoppe' and resistant cultivar 'Sweet Charlie'. The core common DEGs with high association of common DAMs were identified by multi-omics integration analysis, and showed convergence and divergence in the two strawberry cultivars. Strikingly, the phenylpropanoids biosynthesis was simultaneously enriched in a multi-level omics at different stages after *C. fructicola* infection in the resistant (R) and susceptible (S) strawberries. Furthermore, we constructed the DEGs-DAMs map of phenylpropanoid biosynthesis. More importantly, we showed that chloroplasts and starch and sugar metabolism related genes, such as chlorophyll A-B binding genes, glycosyl hydrolase (GH) family genes and so on, were differentially expressed.

Conclusions Taken together, our study revealed major changes in genes and metabolites expression associated with *C. fructicola* resistance, and identified the multi-level regulatory network based on phenylpropanoid biosynthesis, useful for further mechanistic excavation of resistance to *C. fructicola* in strawberries.

Keywords Strawberry, *Colletotrichum fructicola*, Phenylpropanoid, Resistance, Metabolomics

*Correspondence:
Xiaohua Zou
zouxh_113@126.com
Xianping Fang
fxpbio@163.com
[1]Shanghai Key Laboratory of Protected Horticultural Technology, Forestry and Fruit Tree Research Institute, Shanghai Academy of Agricultural Sciences, Shanghai 201403, China

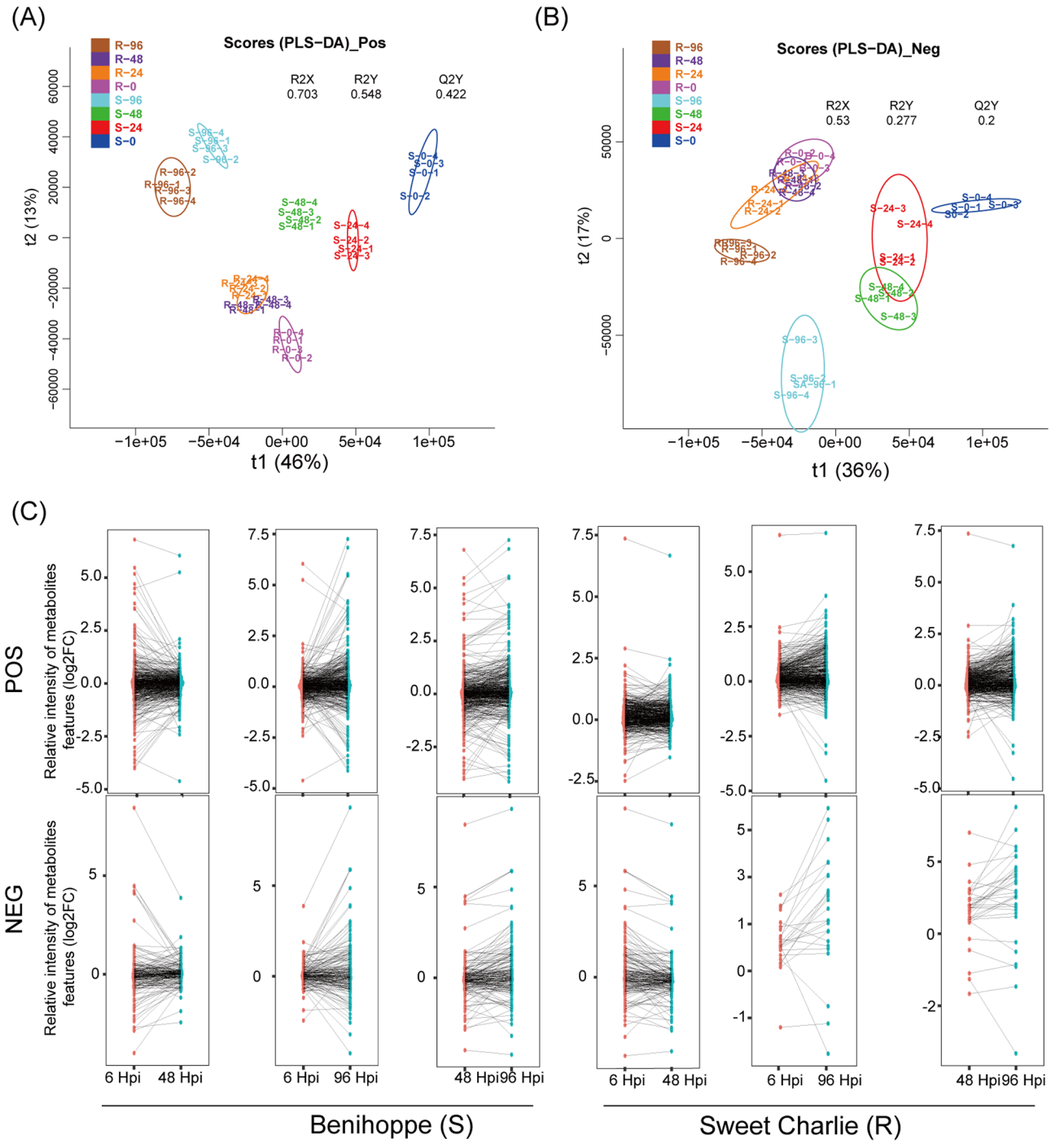

Fig. 1 Differential responses of strawberry cultivars to *C. fructicola* in comparative metabolomics regulation. The PLS-DA analysis of positive ion model (**A**) and negative ion model (**B**) in samples at metabolome. (**C**) The dot plots distribution of fold changes values of metabolites in *C. fructicola*-infected samples compared to the control samples. The lines indicate the patterns of variation between *C. fructicola*- infected samples at different periods after *C. fructicola* inoculation. 'S' represents susceptible 'Benihoppe', 'R' represents resistant cultivar 'Sweet Charlie'

Introduction

The cultivated strawberry (*Fragaria* × *ananassa*) is an important horticultural fruit worldwide, and is popular with consumers because of its flavor and nutrition [1, 2]. Anthracnose is one of the most destructive fungal diseases caused by *Colletotrichum* spp. in cultivated strawberry [3, 4]. Three species, *Colletotrichum acutatum*, *C. fragariae* and *C. gloeosporioides*, as causal agents of strawberry anthracnose have been mainly reported [4–7]. *C. fragariae* causes strawberry

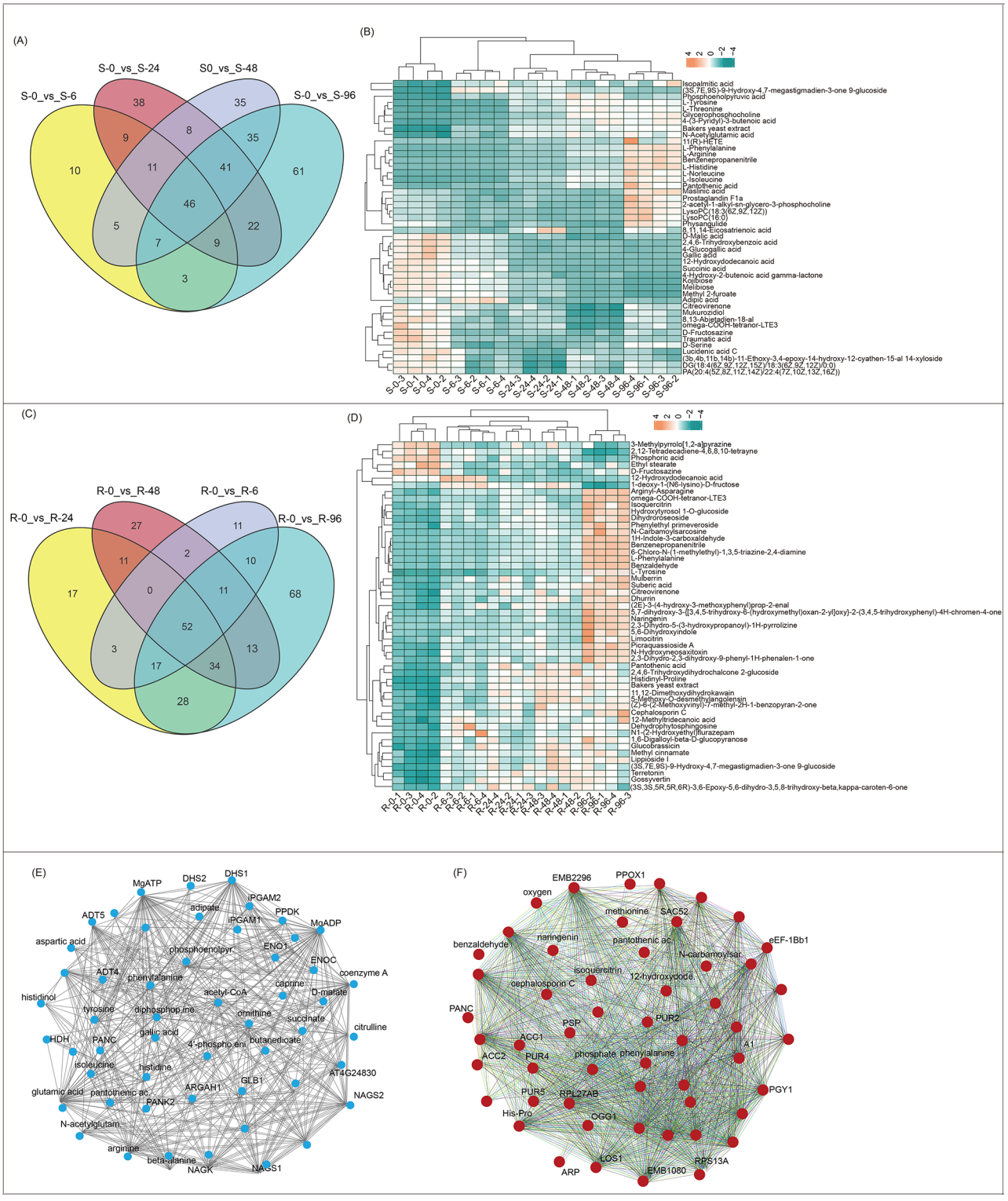

Fig. 2 The accumulation and enrichment of DAMs at different stages after *C. fructicola* inoculation. The venn diagram of common DAMs in 'Benihoppe' (S) (**A**), in 'Sweet Charlie' (R) (**C**) at different stages after *C. fructicola* inoculation. Heatmap of common DAMs in 'Benihoppe' (S) (**B**) and 'Sweet Charlie' (R) (**D**) at different stages after *C. fructicola* inoculation from metabolomics data. Heatmaps demonstrate the relative quantitative mean of all features detected by metabolomics at different stages after *C. fructicola* inoculation. 'S' represents susceptible 'Benihoppe', 'R' represents resistant cultivar 'Sweet Charlie'. The interaction networks show the potential functional relationships between common DAMs at different stages after *C. fructicola* inoculation in 'Benihoppe' (S) (E) and 'Sweet Charlie'(R) (F). The chemical-chemical association for the DAMs network was extracted from STITCH 5

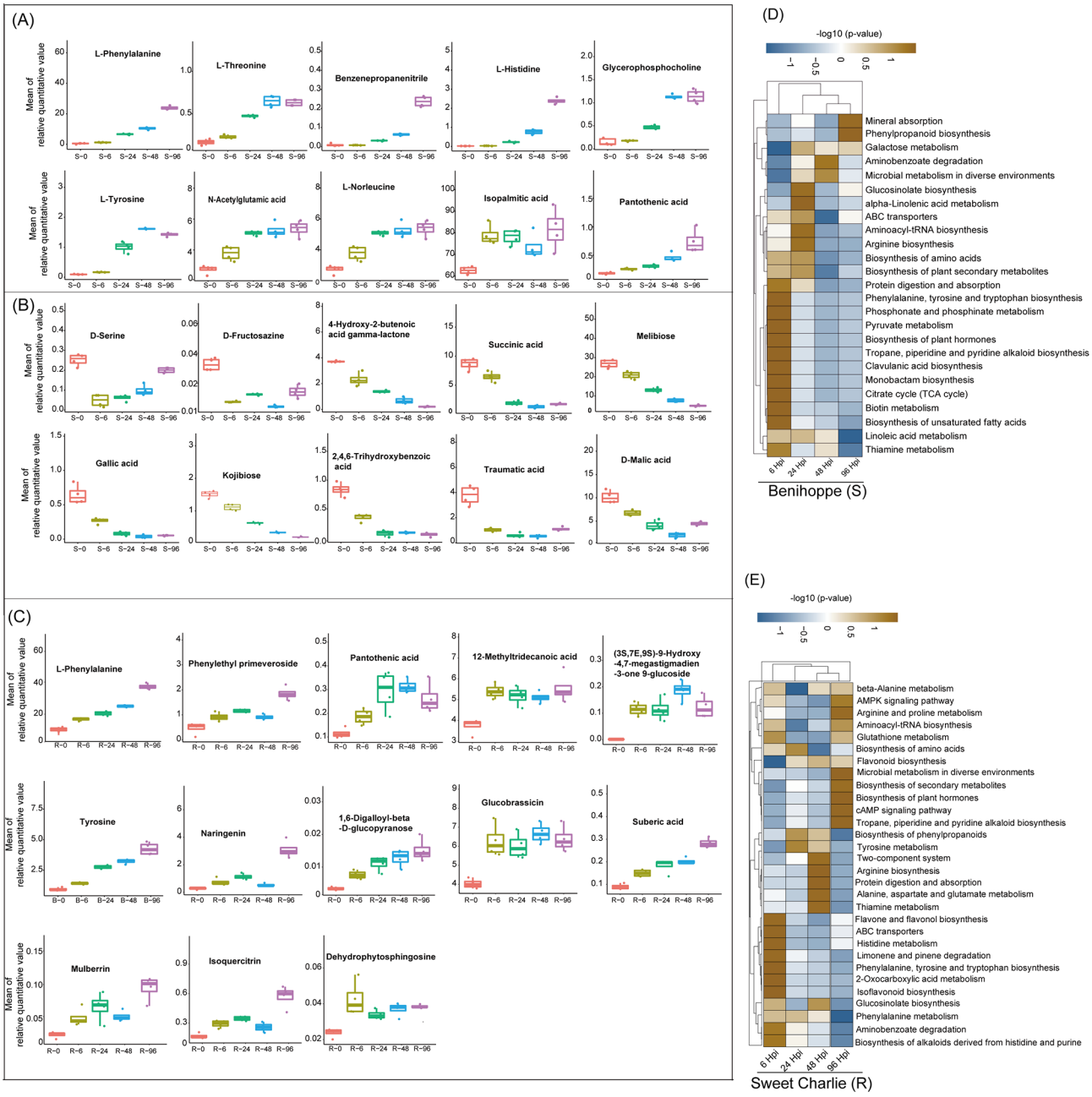

Fig. 3 In-depth metabolomics analysis of DAMs and enriched pathways at different stages after *C. fructicola* inoculation. The boxplots show the mean of relative quantitative value for DAMs detected at different stages after *C. fructicola* inoculation ($P < 0.05$) from 'Benihoppe' up-regulated metabolites (**A**), 'Benihoppe' down-regulated metabolites (**B**) and 'Sweet Charlie' up-regulated metabolites (**C**). Heatmaps show the clustering of commonly enriched pathways in 'Benihoppe' (**D**) and 'Sweet Charlie' (**E**) at different stages after *C. fructicola* inoculation at metabolomics level. Color in heatmap indicating the significant enrichment as -log10 (FDR) in each pathway at different stages after *C. fructicola* inoculation. 'S' represents susceptible 'Benihoppe', 'R' represents resistant 'Sweet Charlie'

anthracnose in the southeastern United States more than 90 years ago. In Europe, the most prevalent species causing anthracnose in strawberry is *C. acutatum* [7]. In Zhejiang province and Shanghai City, *C. fructicola* is the main pathogen causing typical anthracnose symptoms, such as leaf, petiole and stolon lesions, crown rot, or symptoms in the fruit [6, 8].

C. fructicola attacks the strawberry host in a hemibiotrophic infection strategy [9]. Plants have developed complex defense mechanisms to restrain *C. fructicola* infection. *FaNBSs* genes are responsive to *C. fructicola* infection in strawberry [8, 10]. Pathogenesis-related (PR) proteins are up-regulated in strawberry infected with *C. gloeosporioides* [11]. *HSP17.4* participates in

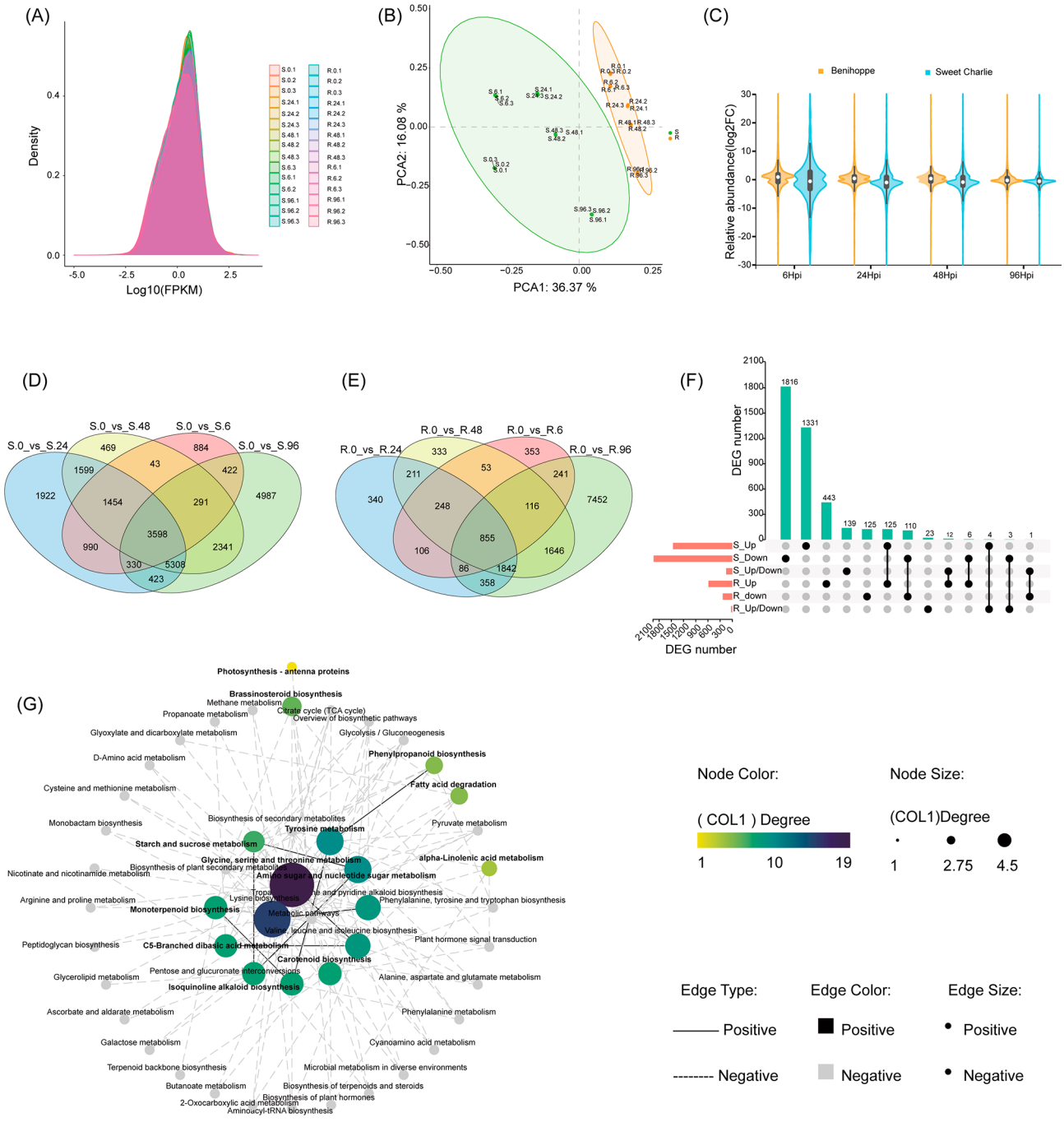

Fig. 4 In-depth analysis of the DEGs and commonly enriched pathways in the transcriptome level at different stages after *C. fructicola* inoculation. All samples detected FPKM value density (**A**) and PCA analysis (**B**). The violin plots show the Fold Change value of samples from different stages after *C. fructicola* inoculation compared with the control group (0 Hpi) (**C**). The Venn diagrams show the number of common DEGs in 'Benihoppe' (**D**) and 'Sweet Charlie' (**E**) at different stages after *C. fructicola* inoculation. The dynamic abundance upset map of DEGs shows the number and expression patterns of DEGs in differentially resistant cultivars (**F**). The pathway enrichment network visualizes the enrichment of common enriched metabolic pathways in differentially resistant cultivars at different stages after *C. fructicola* inoculation in transcriptome level (**G**). The pathway enrichment network was drawn by the omicshare online analysis platform (https://www.omicshare.com/tools/)

the resistance to *C. gloeosporioides* in strawberry [12]. The expression patterns of *FaWRKY* genes are respond to *C. fructicola* inoculation in two ecotype strawberries [13]. Salicylic acid (SA), jasmonic acid (JA), abscisic acid (ABA) and cytokinin signaling pathways are also activated to mediate various cellular responses at the early stage of strawberry/*C. fructicola* interaction [9, 14].

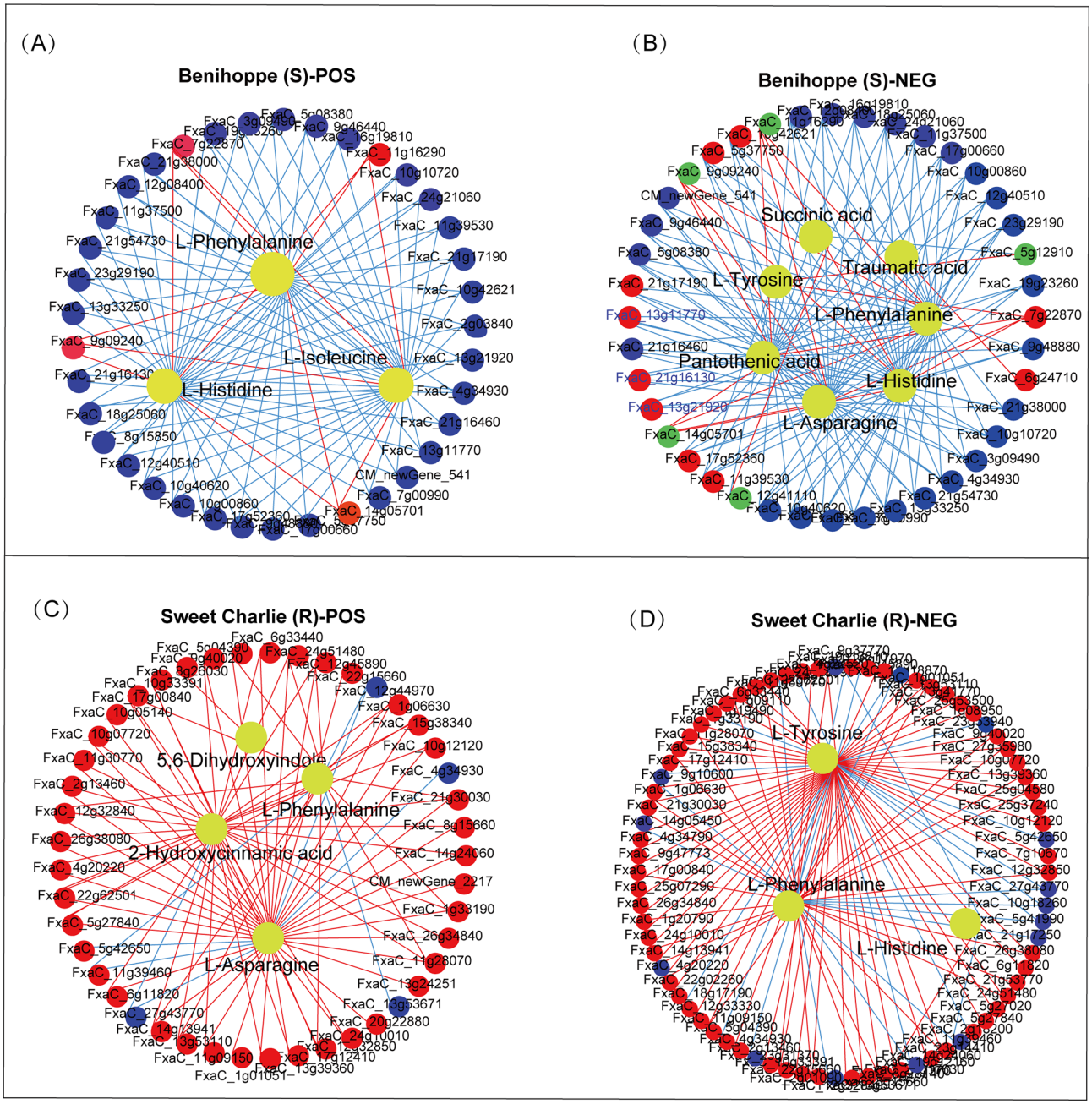

Fig. 5 The co-expression networks between common DEGs and DAMs in differentially resistant strawberry cultivars. Association analysis of the top 100 common DEGs and DAMs (p-value < 0.01, $R^2 > 0.9$) in 'Benihoppe' (**A**-**B**), and 'Sweet Charlie' (**C**-**D**) at different stages after *C. fructicola* inoculation. The yellow dots represent DAMs, and the red, blue and green dots represent the three possible relationships of DAMs to DEGs. The red line represents a positive correlation, and the blue line represents a negative correlation. 'POS' represents the positive ion model, and 'NEG' represents the negative ion model. 'S' represents susceptible 'Benihoppe', 'R' represents resistant cultivar 'Sweet Charlie'. The top 100 common DAMs and DEGs in different cultivars at different stages after *C. fructicola* inoculation with p-value > 0.9 and $R^2 > 0.9$ were screened for correlation analysis

The interactions between *C. fructicola* and strawberries have been reported [15]. Transcriptomic studies have been reported to investigate the effects of strawberry responses to *C. fructicola* and *C. gloeosporioides* [10, 11]. Previously, we have analyzed the resistance to *C. fructicola* by transcriptome analysis in 'JiuXiang' [10]. Nevertheless, there are no reported study on comparative metabolomics and transcriptomics analysis of *C. fructicola* resistance in strawberries. In this study, we used the susceptible 'Benihoppe' and resistance cultivar 'Sweet Charlie' [16, 17] to generate metabolomics and transcriptomics data and elucidate the defense response of strawberries to *C. fructicola* infection. In addition, we uncovered the complex metabolic pathway network

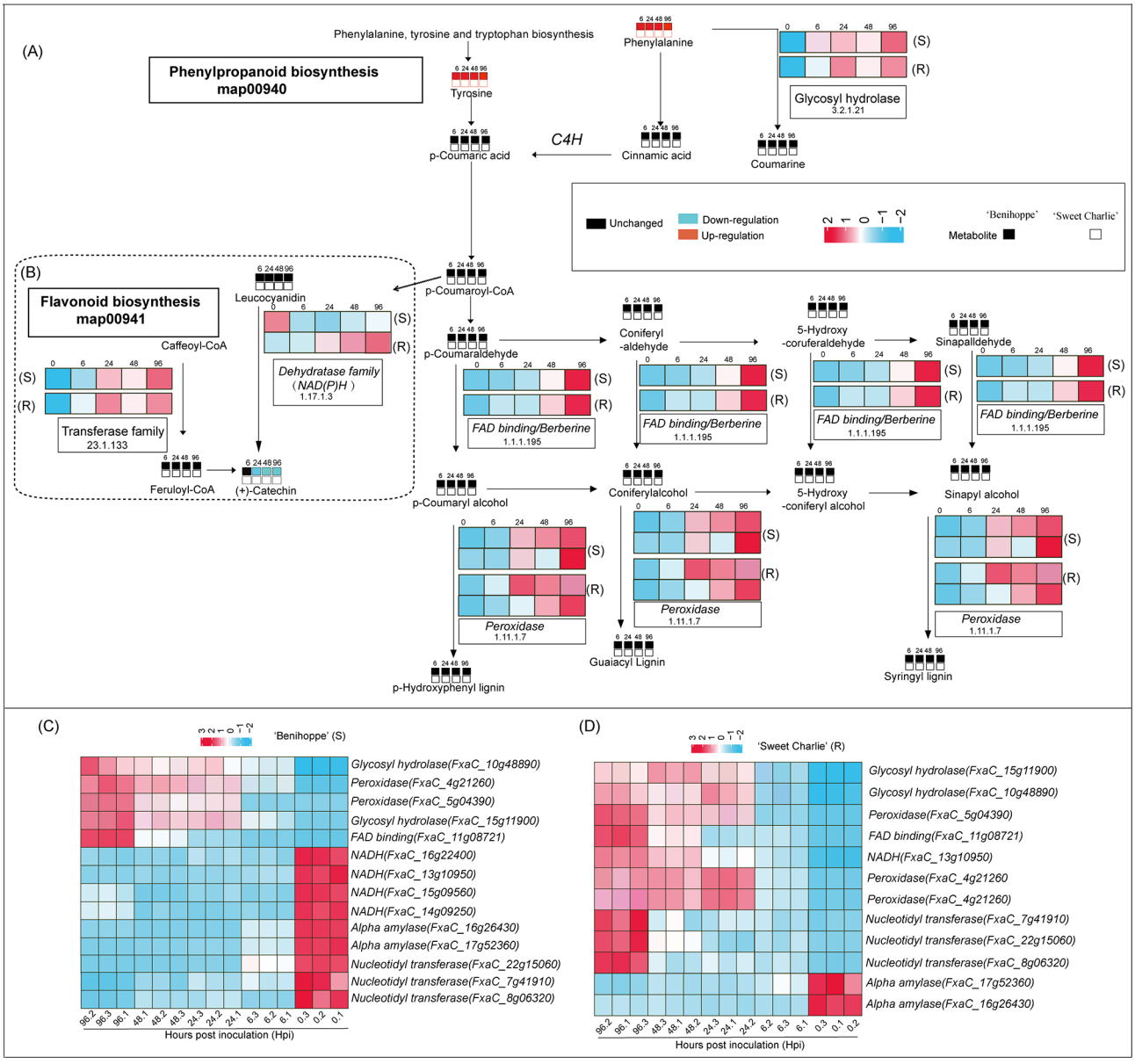

Fig. 6 Different expressions of structural genes and metabolites in phenylpropanoid biosynthesis related pathway in resistant and susceptible strawberry cultivars after *C. fructicola* inoculation. The simplified metabolic flow charts show the changes of DEGs and DAMs enriched in phenylpropanoid biosynthesis (**A**) and flavonoid biosynthesis (**B**). The red and blue blocks represent up-regulation and down-regulation of expression, respectively. The Black blocks represent unchanged expression. The blocks with filled colour represent 'Benihoppe', the blocks without filled colour represent 'Sweet Charlie'. The heatmap representation of phenylpropanoid biosynthesis -related DEGs expression patterns in 'Benihoppe' (**C**) and 'Sweet Charlie' (**D**). The gene expression data are shown as a heatmap depicting log2 (FPKM) values

dominated by phenylpropanoid synthesis in regulating *C. fructicola* resistance. Results reported herein will deepen the understanding of the anthracnose resistance mechanism in octoploid strawberries.

Materials and methods

Plant materials, inoculation and sampling

Two octoploid strawberries, namely 'Sweet Charlie' (Resistant, R) and 'Benihoppe' (Susceptible, S) with the same genomic background, were used in this study. In detail, the seedlings developed from stolons through asexual reproduction, were cultivated from a nursery in pots with sterilized substrate in greenhouse for 3 months.

The pathogen of *C. fructicola* isolate (CGMCC3.17371) was used in our study [8]. The method of cultivation and inoculation was described as previous paper [9, 10]. Briefly, *C. fructicola* was activated on the solid PDA medium at 28 °C. Then, the conidia were propagated and suspended in liquid PDA medium at 28 °C, 220 rpm. The spore density of 1×10^6 spores per mL with 0.01% (v/v)

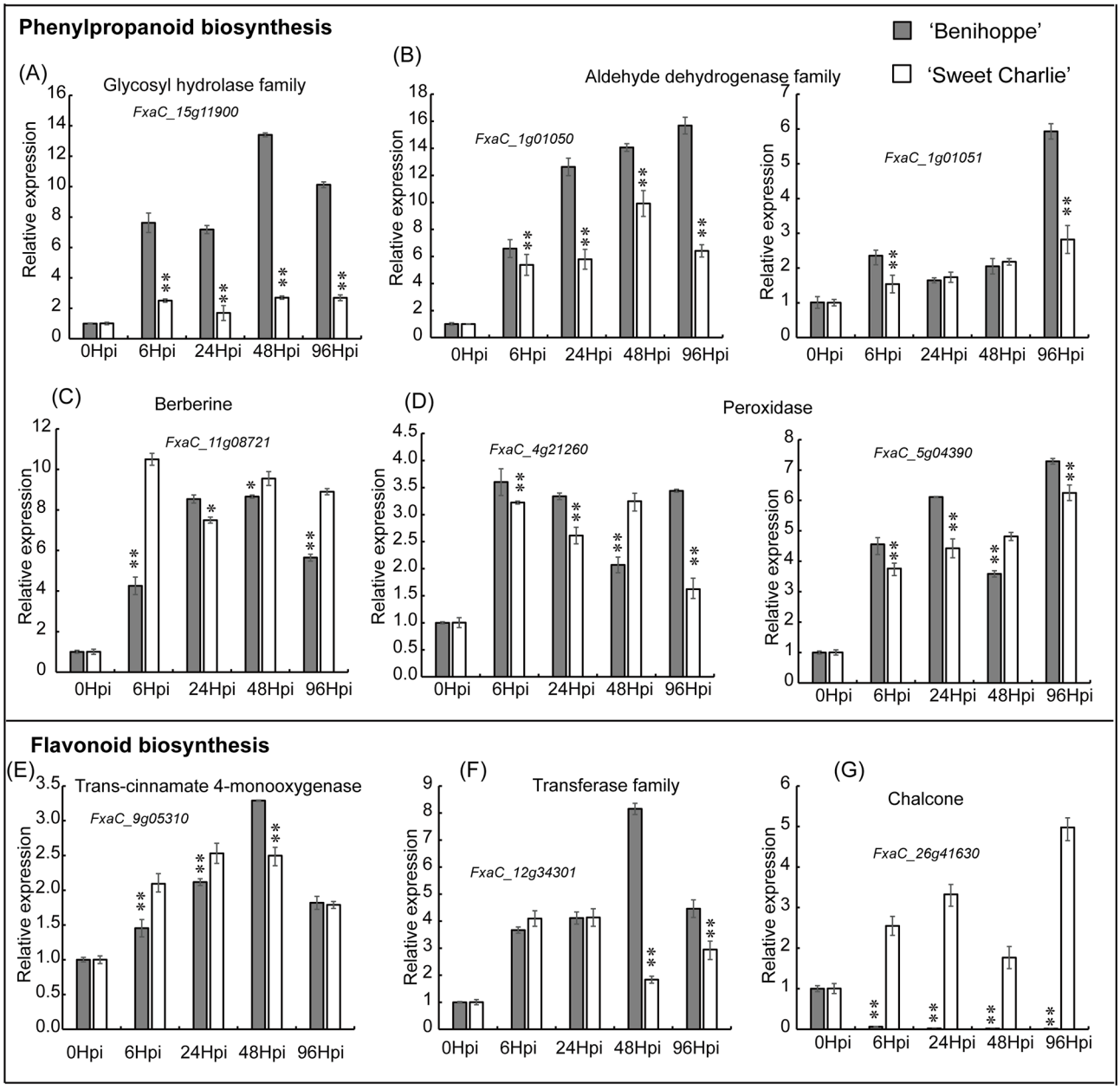

Fig. 7 Expression profiles of common DEGs in phenylpropanoid biosynthesis related pathway after *C. fructicola* infection by qRT-PCR analysis. The 3-5th compound leaves of strawberry 'Benihoppe' and 'Sweet Charlie' were sampled at 0 (Mock), 6, 24, 48 and 96 h post inoculation (Hpi). For qPCR analysis, the relative mRNA levels of each gene were normalized with respect to the most stable transcripts *FaCHP1* at the different stages. Data are shown as means ± SD (Student's t tests, $^{**}P < 0.01$, $n = 3$)

Tween 20 in sterile water was used to spray the strawberry leaves. Mock inoculations of plants were sprayed using just the Tween 20 water solution [17]. Leaf samples were harvested at 0, 6, 24, 48 and 96 h post inoculation (Hpi) respectively. In detail, the 3rd-5th fully expanded compound leaves, collected from eight independent plants at each time point were pooled as a biological replicate. Four independent biological replicates were sequenced for each treatment.

Analysis of disease assessment

The disease symptoms were indicated by any sign of disease spots on the leaves. Five leaves chosen at random in each plant were scored for symptom development from 3, 5, 8, 10, 12 and 14 day post-inoculation (Dpi). The severity of symptoms is expressed as disease index and leaf incidence. Leaf lesions were grouped into five scales according to the percentage of observed spots as follows: 0 = healthy leaf, no disease spots; 1 ≦ 5% disease spots area on the compound leaves; 2 = 5–10% disease spot

area; 3 = 10–15% disease spot area; 4 = 15–20% disease spot area; 5 = > 20% disease spot area [11, 17]. The disease index (DI) was calculated according to the formula DI = (∑(N × V)/N × Z) × 100%, where N is the lesion score class, V is the number of samples in the score class, N is the highest score value, and Z is the total number of samples.

RNA extraction, qualification, library preparation and sequencing

Total RNA was extracted using RNAiso Plus (total RNA extraction reagent) (TaKaRa, Otsu, Japan). The degradation and contamination of RNA were monitored on 1% agarose gels. RNA purity was checked using the NanoPhotometer® spectrophotometer (IMPLEN, CA, USA). RNA integrity was assessed using the RNA Nano 6000 Assay Kit of the Bioanalyzer 2100 system (Agilent Technologies, CA, USA). The libraries of transcriptome sequencing were generated using NEBNext® UltraTM RNA Library Prep Kit for Illumina® (NEB, USA). The library quality was assessed on the Agilent Bioanalyzer 2100 system. The clustering of the index-coded samples was performed on a cBot Cluster Generation System using TruSeq PE Cluster Kit v3-cBot-HS (Illumia). The library preparations were sequenced on an Illumina Novaseq platform and 150 bp paired-end reads were generated. Illumina raw reads data quality was verified with Fastp (v0.20.0) and then compared to the reference genome of *Fragaria ×ananassa* Camarosa (v1.0.a2, a re-annotation of v1.0.a1) using HISAT2 (v2.1.0). The transcript was assembled by StringTie (stringtie-2.1.3b. Linux_x86_64) software according to the bam file.

Gene expression analysis and function annotation

The read count matrix of gene expression was conducted using Ballgown (R script). The analysis of DEGs was performed using the DESeq2 software (R script). The DEGs in pair-wise comparisons were defined with |Log2FC | ≥ 1 with FDR ≤ 0.05. R (v3.6.2) ggplot2 package was used to draw MA diagrams, volcano diagrams and box diagrams. BLASTALL (v2.2.26) software was employed to annotate GO, KEGG, COG, KOG, NR, Swissprot and Pfam databases for the DEGs.

Expression analysis using real-time quantitative PCR (qPCR)

The method of qPCR experiment was described as previous paper in our laboratory [13]. The relative mRNA levels of each gene were normalized with respect to the strawberry most stable transcripts *FaCHP1* (contig 21335) [18]. As an independent validation, the samples of qPCR were harvested at 0, 6, 24, 48 and 96 Hpi respectively. Three independent biological replicates were sequenced for qPCR experiment. The qPCR primers were listed in Table S1.

Metabolites extraction and LC-MS/MS analysis

Freeze-dried samples (50 mg) were extracted with 1000 μL of an extract solution containing methanol, acetonitrile and water (2:2:1 v: v:v), and an isotopically-labelled internal standard mixture. Then the samples were homogenized at 35 Hz for 4 min and sonicated for 5 min in ice-water bath. Then the samples were incubated for 1 h at -40 ℃ and centrifuged at 12,000 rpm for 15 min at 4 ℃. The supernatants were transferred to fresh glasses vial for analysis. The quality control (QC) sample was prepared by mixing an equal aliquot of the supernatants from each sample.

LC-MS/MS analyses were performed using an UHPLC system (Vanquish, Thermo Fisher Scientific) with a UPLC BEH Amide column (2.1 mm × 100 mm, 1.7 μm) coupled to Q Exactive HFX mass spectrometer (Orbitrap MS, Thermo). The mobile phase consisted of 25 mmol/L ammonium acetate and 25 mmol/L acetic acid in water (A) and acetonitrile (B). The auto-sampler temperature was 4 ℃, and the injection volume was 2 μL. The QE HFX mass spectrometer was used for its ability to acquire MS/MS spectra on information-dependent acquisition (IDA) mode in the control of the acquisition software (Xcalibur, Thermo). In this mode, the acquisition software continuously evaluates the full scan MS spectrum. The ESI source conditions were set as following: sheath gas flow rate as 30 Arb, Aux gas flow rate as 25 Arb, capillary temperature 350 ℃, full MS resolution as 60,000, MS/MS resolution as 7500, collision energy as 10/30/60 in NCE mode, spray Voltage as 3.6 kV (positive) or -3.2 kV (negative), respectively.

The raw data was converted to the mzXML format using ProteoWizard and processed with an in-house program, which was developed using R for peak detection, extraction, alignment, and integration. Then MS2 database was applied in metabolite annotation. The cutoff for annotation was set at 0.3. The multivariate analysis of identified metabolites was performed using orthogonal projections to latent structures- discriminant analysis (OPLS-DA). Metabolites with VIP > 1, P-value < 0.05 and FC ≥ 1.2 or FC ≤ 0.8 were considered differentially regulated.

Integrated analysis of transcriptome and metabolome

Spearman correlations were calculated using the psych package in R (v3.6.2) between the top 100 DAMs and DEGs at different stages after *C. fructicola* inoculation, or the common DAMs and DEGs in the same pathway. The selection criteria were the value of correlation > 0.9 and p value < 0.001. Cytoscape software (Cytoscape

Consortium, USA, version 3.8.0) was used to visualize the interaction networks between DEGs and DAMs.

Data statistical analysis

Principal component (PCA) analysis was assessed using the software SIMCA in the QC samples and experimental samples. Pearson correlation coefficient (PCC) analysis and relative standard deviation (RSD) analysis were performed using the R (V3.6.2) corrplot and plotrix packages. Correlation heat maps and RSD distributions were plotted.

Results

Differential responses of two octoploid strawberries to *C. fructicola*

In China, 'Sweet Charlie' and 'Benihoppe' are two predominant octoploid strawberry cultivars nationwide, which belong to the same species [19, 20]. Many reports have confirmed the typical resistance differences between 'Sweet Charlie' and 'Benihoppe' to *C. fructicola* infection. Here, by observing symptoms of leaves and DIs, we also verified that 'Sweet Charlie' was resistant to *C. fructicola* infection and 'Benihoppe' was susceptible to *C. fructicola* infection (Fig. S1). This result is consistent with previous research [12, 13].

Metabolite profiling of resistant and susceptible octoploid strawberries in response to *C. fructicola* infection

We performed a non-targeted liquid chromatography-mass spectrometry (LC-MS) analysis with 4 replicates in the resistant (R) 'Sweet Charlie' and susceptible (S) 'Benihoppe' strawberries at 4 different time points after *C. fructicola* inoculation to generate a metabolomics data set. After pretreatment, there were 498 and 171 metabolites were detected in positive (POS) and negative (NEG) ion model, respectively (Fig. S2). In both 'Benihoppe' and 'Sweet Charlie', for metabolites at control group (0 Hpi) and different stages after *C. fructicola* inoculation (6, 24, 48 and 96 Hpi), we evaluated their distinction between *C. fructicola*-infected samples and healthy control samples by principal component analysis (Fig. 1A, B). To determine the metabolite changes induced by *C. fructicola* inoculation in octoploid strawberries, we analyzed the $\log_2$-fold changes of metabolite components between different stages after *C. fructicola* inoculation by compared with the 0 Hpi control samples. The results showed that many metabolite components were differentially accumulated at different stages after *C. fructicola* in the resistant (R) and susceptible (S) strawberries (Fig. 1C).

Identification of DAMs after *C. fructicola* infection in resistant (R) and susceptible (S) strawberries

Further, we analyzed the DAMs between sample pairs after *C. fructicola* inoculation (6 Hpi vs. 0 Hpi, 24 Hpi vs. 0 Hpi, 48 Hpi vs. 0 Hpi and 96 Hpi vs. 0 Hpi) in the resistant (R) and susceptible (S) strawberries. We found that there were 46 and 52 common DAMs among different stages after *C. fructicola* infection in the susceptible 'Benihoppe' and resistant 'Sweet Charlie' respectively (Fig. 2A, C). The relative expression patterns of common DAMs in 'Benihoppe' and 'Sweet Charlie' were shown in heatmaps. What's more, we revealed the specifically up-regulated DAMs in susceptible 'Benihoppe' after *C. fructicola* inoculation, such as L-tyrosine, L-threonine, L-histidine, L-noreucine, maslinic acid, and so on (Fig. 2B). In the resistant 'Sweet Charlie', most of the common DAMs showed up-regulated accumulation after *C. fructicola* inoculation compared with control group (0 Hpi) (Fig. 2D).

Based on the known reactions in PubMed, using STITCH 5 [21], we generated a predictive network to uncover the metabolite-metabolite interactions within the common DAMs between two strawberry cultivars. In detail, the common DAMs associated with amino acids, acetyl-CoA, phenylalanine and organic acids were influenced in 'Benihoppe' (Fig. 2E). Meanwhile, the common DAMs associated with methionine and phenylalanine were influenced in 'Sweet Charlie' (Fig. 2F).

Furthermore, we analyzed the expression patterns of DAMs at different stages after *C. fructicola* inoculation. There were ten up- and ten down-regulated metabolite compounds in the 'Benihoppe' (Fig. 3A, B). Meanwhile, in the 'Sweet Charlie', there were 13 metabolite compounds were up- accumulated at different stages after *C. fructicola* infection (Fig. 3C). More importantly, L-phenylalanine, as a core metabolite, was significantly induced in susceptible 'Benihoppe' and resistant 'Sweet Charlie' at different stages after *C. fructicola* inoculation.

In addition, we analyzed the convergence of enriched pathways in each cultivar based on the common DAMs after *C. fructicola* inoculation. At the metabolome level, we identified 25 and 30 commonly enriched (P-value < 0.05) pathways in 'Benihoppe' and 'Sweet Charlie' cultivars respectively. The co-enriched pathways in the resistant (R) and susceptible (S) strawberries were identified as biosynthesis of phenylpropanoids, phenylalanine metabolism, biosynthesis of plant hormones, glucosinolate biosynthesis, aminoacyl-tRNA biosynthesis, ABC transporters, biosynthesis of amino acids, thiamine metabolism, biosynthesis of plant secondary metabolites (Fig. 3D, E). Moreover, the pathways specific enriched pathways in 'Benihoppe' were monobactam biosynthesis, linoleic acid metabolism, Citrate cycle (TCA cycle), biosynthesis of unsaturated fatty acids, galactose metabolism, alpha-linolenic acid metabolism and pyruvate metabolism (Fig. 3D). Conversely, the specific enriched pathways in 'Sweet Charlie' were AMPK signaling pathway, cAMP signaling pathway, flavonoid and flavonol

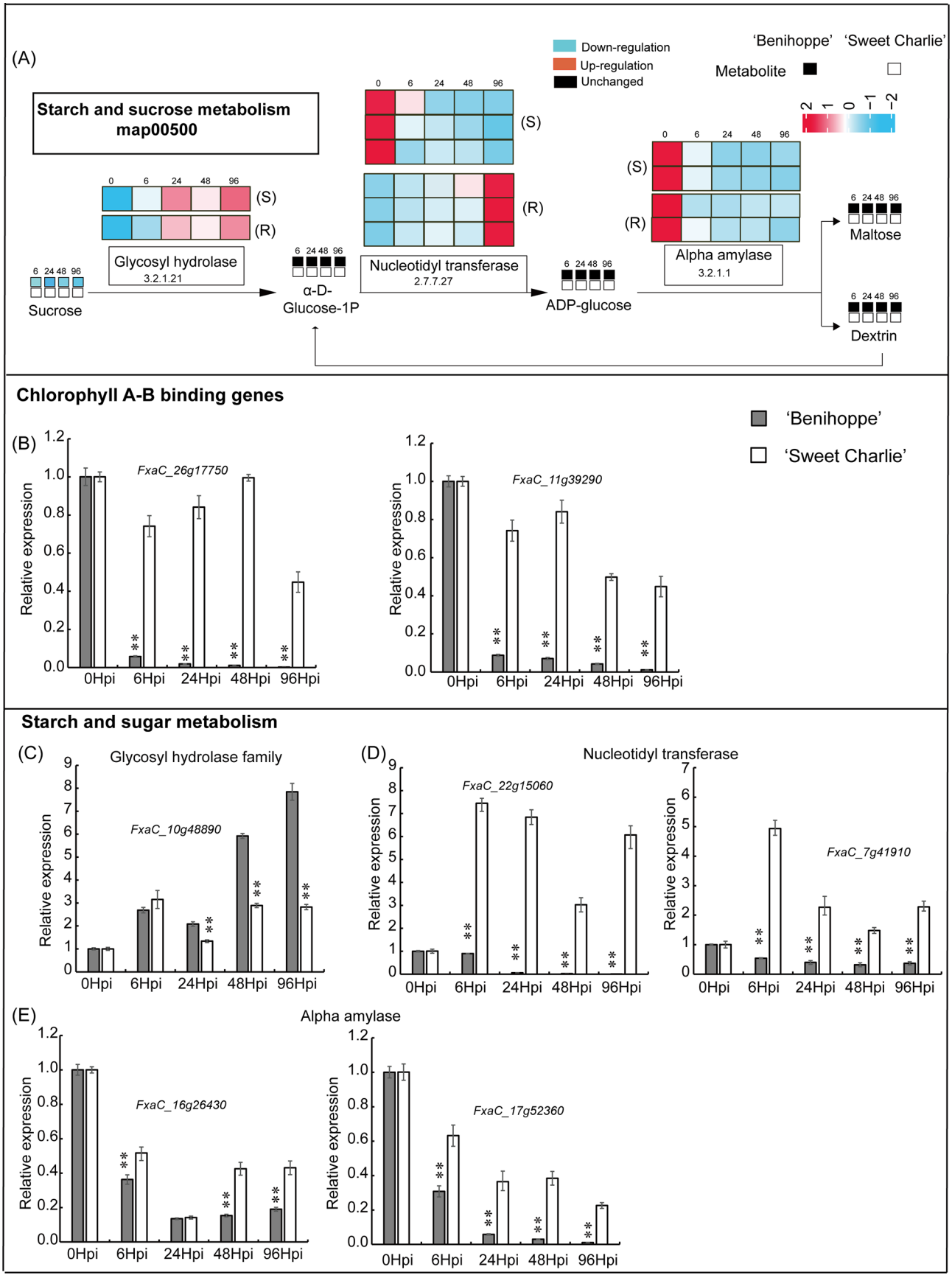

Fig. 8 (See legend on next page.)

(See figure on previous page.)

Fig. 8 Starch and sugar metabolism pathway in strawberry after *C. fructicola* infection. Expression profiles of common DEGs and DAMs in starch and sugar metabolism pathway after *C. fructicola* infection. The simplified metabolic flow charts show the changes of DEGs and DAMs enriched in starch and sucrose metabolism (**A**). The qRT-PCR analysis shows the expression pattern of common DEGs for chlorophyll A-B binding genes (**B**) and starch and sugar metabolism(**C**-**E**). The 3th, 4th and 5th compound leaves of strawberry 'Benihoppe' and 'Sweet Charlie' were sampled at 0 (Mock), 6, 24, 48 and 96 h post inoculation (Hpi). For qPCR analysis, the relative mRNA levels of each gene were normalized with respect to the most stable transcripts *FaCHP1* at the different stages. Data are shown as means ± SD (Student's t tests, $^{**}P < 0.01$, $n = 3$)

biosynthesis, flavonoid biosynthesis, glutathione metabolism, histidine metabolism, isoflavone biosynthesis, 2-oxocarboxylic acid metabolism, and tyrosine metabolism (Fig. 3E). These commonly and specifically enriched pathways may highlight the characteristics of DAMs in strawberry responding to *C. fructicola* at metabolomic level.

Transcriptome profiles of resistant and susceptible octoploid strawberries in response to *C. fructicola* infection

Meanwhile, we studied the changes of gene expression profiles among the both octoploid strawberries at different stages after *C. fructicola* inoculation by comparing transcriptomes (Fig. 4). Therefore, by aligning the clean reads to the strawberry reference genome (*Fragaria* × *ananassa Camarosa* Genome v1.0.a2 (Re-annotation of v1.0.a1)) (Table S2). We evaluated the overall distribution of RPKM values (Fig. 4A), and the data quality was validated by principal component analysis (Fig. 4B). Using the co-expressed gene sets from the transcriptome data, the different modules were divided by WGCNA analysis (Fig. S3). To determine the changes of DEGs induced by *C. fructicola* infection in strawberry, we performed $\log_2$-fold comparisons of 4 pairs of data sets with 0 Hpi controls at different stages after *C. fructicola* inoculation in the two cultivars (Fig. 4C). Also, we obtained 3598 and 855 overlapped DEGs in different stages after *C. fructicola* in both cultivars, respectively (Fig. 4D, E). Further, we analyzed the expression patterns of core DEGs, and found that there were 1331 core DEGs up-regulated and 1816 core DEGs down-regulated in 'Benihoppe'. Meanwhile, there were 443 core DEGs up-regulated and 125 core DEGs down-regulated in 'Sweet Charlie'. Besides, there were 125 common DEGs up-regulated and 110 common DEGs down-regulated in the both cultivars at different stages after *C. fructicola* inoculation (Fig. 4F), which may be responsive to *C. fructicola* resistance in strawberry. What's more, at the transcriptional level, we also identified the significantly enriched pathways (P-value < 0.05) in the resistant (R) and susceptible (S) strawberries at different stages after *C. fructicola* inoculation, such as photosynthesis-antenna proteins, phenylpropanoid biosynthesis, starch and sucrose metabolism, glucosinolate biosynthesis, fatty acid degradation, tyrosine metabolism, isoquinoline alkaloid biosynthesis, glutathione metabolism, alpha-linolenic acid metabolism and monoterpenoid biosynthesis (Fig. 4G). We speculate that these commonly enriched pathways may induce the defense responses in the resistant (R) and susceptible (S) strawberries after *C. fructicola* inoculation at the transcriptome level.

Integrated analysis of common DAMs and DEGs in response to *C. fructicola* inoculation

To further explore the resistance defense mechanism in strawberry after *C. fructicola* infection, we integrated the transcriptome and metabolome datasets based on the common DAMs and DEGs in each cultivar respectively. The co-expression networks were constructed in each cultivar at different stages after *C. fructicola* infection. Firstly, we found that the common DAMs (including L-phenylalanine, L-histidine, succinic acid, traumatic acid, L-tyrosine, pantothenic acid, L-histidine, L-asparagine) were negatively correlated with the most of DEGs (Fig. 5A, B) at different stages after *C. fructicola* infection in susceptible 'Benihoppe'. Subsequently, we also found that the common DAMs (including 5,6-dihydroxyindole, L-phenylalanine, 2-hydroxycinnamic acid, L-asparagine, L-tyrosine, L-histidine and L-phenylalanine) were positively correlated with most of the common DEGs at different stages after *C. fructicola* infection in resistant 'Sweet Charlie' (Fig. 5C, D). We speculate that the responses of common DAMs may be distinctive, but L-phenylalanine is convergently enriched in the resistant (R) and susceptible (S) strawberry cultivars.

Reprogramming of the phenylpropanoid biosynthesis related pathways in response to defense against *C. fructicola*

Many secondary metabolites derived from the phenylpropanoid pathway are important components in regulating plant defense immune [22]. At the transcript level, we found that the expression patterns of core DEGs in phenylpropanoid biosynthesis related pathways were activated at different stages after *C. fructicola* infection in the two differentially resistant strawberry cultivars, including the genes encoding berberine (*FxaC_11g08721*) (Figs. 6A and 7C), aldehyde dehydrogenase (*FxaC_1g01050*, *FxaC_1g01051*) (Fig. 7B), and peroxidase (*FxaC_5g04390*, *FxaC_4g21260*) (Figs. 6A and 7D). Furthermore, the expression of glycosyl hydrolase genes was significantly up-regulated by RT-PCR experiments (Figs. 6C, 7A and 8C).

Flavonoids consist of many secondary metabolites related to phenylpropanoid pathway, and they act as a significant role in stress response [23, 24]. Coincidentally, the genes coding for dehydratase family (*FxaC_13g10950*), involved in flavonoid biosynthesis, were induced in the resistant 'Sweet Charlie' compared to susceptible 'Benihoppe' (Fig. 6C-D). The transferase family genes (*FxaC_12g34301*) were also induced in the both strawberries after *C. fructicola* infection (Fig. 7F). Also, we verified the genes encoding trans-cinnamate 4-monooxygenase (*FxaC_9g05310*) was significantly up-regulated in transcriptome level at different stages after *C. fructicola* infection in the two differentially resistant cultivars (Fig. 7E). More importantly, we proved that the expression of catechin biosynthesis gene (*FxaC_26g41630*) was induced in resistant 'Sweet Charlie' and inhibited in susceptible 'Benihoppe' at different stages after *C. fructicola* infection (Fig. 7G). In addition, at the metabolome level, the catechin was also inhibited in susceptible 'Benihoppe' at different stages after *C. fructicola* infection (Fig. 6B).

Meanwhile, we found that the expression of Chlorophyll A-B binding genes (*FxaC_26g17750*, *FxaC_11g39290*) showed a sharp down-regulation after *C. fructicola* infection in susceptible 'Benihoppe' (Fig. 8B). In starch and sugar metabolism, the glycosyl hydrolase family gene (*FxaC_10g48890*) was up-regulated in differentially resistant strawberry cultivars. The expression of Nucleotidyl transferase genes (*FxaC_22g15060*, *FxaC_7g41910*) was activated in the resistant 'Sweet Charlie' and inhibited in the susceptible 'Benihoppe' (Fig. 8D). The Alpha amylase (*FxaC_16g26430*, *FxaC_17g52360*) was down-regulated after *C. fructicola* infection (Fig. 8A, E).

Discussion

Anthracnose is one of the most harmful fungal diseases in strawberry. Previous studies have revealed the molecular mechanism of interaction between strawberry and *C. gloeosporioides* by transcriptomics [10, 11]. In this study, we used the representative resistant 'Sweet Charlie' and susceptible 'Benihoppe' to systematically elucidate the defense mechanism through multi-omics analysis of metabolomics and transcriptomics datasets after being infected with C. *fructicola*. Our analysis summarized the common and specific defense strategies of differentially resistant cultivars after *C. fructicola* infection at multi-omics level, which may effectively explain the dynamic changes and processes in metabolic pathways related to *C. fructicola* resistance in differentially resistant strawberry cultivars.

In strawberry after *C. fructicola* infection, the expression of phenylpropanoid pathway related genes showed differences in differentially resistant strawberry cultivars. Phenylpropanoids are essential for effective immune responses in plant [25–28], which modulate the resistance of *Sclerotinia sclerotiorum* in soybean [29]. Here, phenylpropanoid biosynthesis is an important pathway involved in *C. fructicola* defense. Combined with the results of multi-omics, we reveal that the responses to *C. fructicola* at transcriptome and metabolome in a very similar manner by convergent enrichment of phenylpropanoid biosynthesis in differentially resistant strawberry cultivars (Figs. 2, 3 and 4).

At the metabolome level, phenylalanine and tyrosine are more induced in resistant 'Sweet Charlie' than in susceptible 'Benihoppe' at different stages after *C. fructicola* infection. Phenylalanine can induce tomato resistance to Tuta absoluta by positively regulating the accumulation of benzenoid/phenylpropanoid volatiles [30]. Phenylalanine ammonia lyase (PAL) gene plays an important role in SA-dependent defense response [31]. Although the highest level of phenylalanine is detected in differentially resistant strawberry cultivars at 96 Hpi (Fig. 3A, B), the content of phenylalanine is significantly higher in resistant 'Sweet Charlie' than in susceptible 'Benihoppe' at each time point after *C. fructicola* infection, which may be more conducive to stimulating SA-dependent defenses in resistant 'Sweet Charlie' (Fig. 9).

Secondary metabolites, such as lignin, isoflavone phytoalexin precursors, and other phenolic compounds in multiple branches of phenylpropanoid biosynthesis, are important components of plant defense responses [32–35]. We speculate that the differentially accumulated phenylalanine, tyrosine and other metabolites, combined with the differentially expressed downstream defense response-related genes, including berberine, peroxidase, glycosyl hydrolase family, aldehyde dehydrogenase, trans-cinnamate 4-monooxygenase, 4-coumarate-CoA and oxygenase superfamily, may participate in the defense responses to *C. fructicola* in octoploid strawberries. The role of these DEGs and DAMs in resistance to *C. fructicola* provide a kind of clue for our future research.

The genes and metabolites in starch and sugar metabolic pathways showed differentially accumulated after *C. fructicola* infected octoploid strawberries. The sugar metabolism and phenylpropanoid pathway affect the disease resistance of peach fruits by inhibition of hexokinase activity [36]. The glycosyl hydrolase genes are involved in both starch and sucrose metabolism and phenylpropanoid biosynthesis [37]. Here, the expression of starch and sucrose metabolism related genes, such as glycosyl hydrolase family genes, nucleotidyl transferase and alpha amylase, have different responses to *C. fructicola*. In the susceptible 'Benihoppe', the glycosyl hydrolase genes is earlier and more induced. The glycosyl hydrolase family proteins play an important role in the degradation of the host's cell wall [38, 39]. The earlier induced expression of glycosyl hydrolase genes in susceptible 'Benihoppe' may

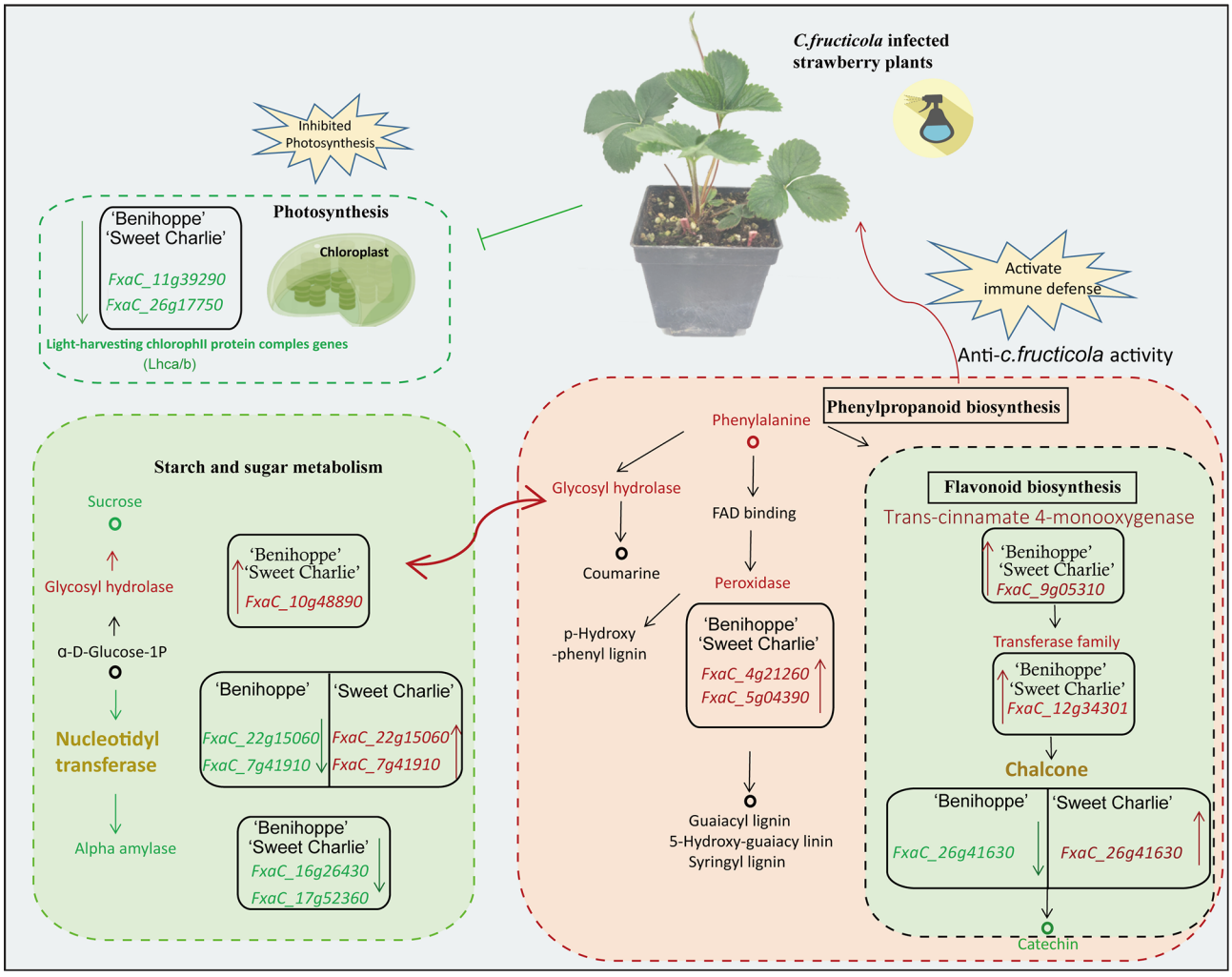

Fig. 9 A proposed model of strawberry in response to *Colletotrichum fructicola* resistance

be more beneficial to break the strawberry cell wall for *C. fructicola* infection. Nucleotidyl transferases are common transferases and play a crucial role in stress responses, and disease resistance [40]. Here, the expression pattern of nucleotidyl transferase genes presents a positive correlation with the strawberry defence against *C. fructicola* infection, which might participate in defensive reaction and provide a possibility for the defense against *C. fructicola* in octoploid strawberries (Fig. 9).

Plant pathogens have convergently evolved to target chloroplasts and impair SA-dependent defenses. There is a pathway linking plasma membrane to chloroplasts and activating defense exists in plants, which has been co-opted by plant pathogens during host-pathogen co-evolution to promote virulence through suppression of SA responses [41–43]. Here, the expression patterns of chlorophyll A-B binding genes were significantly down-regulated at different stages after *C. fructicola* infection in differentially resistant strawberry cultivars (Fig. 9). It is important to mention that the expression of chlorophyll A-B binding genes was dramatically reduced in the susceptible 'Benihoppe' than in the resistant 'Sweet Charlie'. Salicylic acid (SA) can present a very early burst at 1 h post inoculation *C. fructicola* in strawberry [9]. The SA-dependent defenses may be greatly weakened in the susceptible 'Benihoppe' by rapidly reducing the chlorophyll A-B binding genes in the early Strawberry/*C.fructicola* interaction. In the resistant 'Sweet Charlie', the process of enhancing virulence by inhibiting SA-dependent defenses through chloroplasts might be delayed and weaken. Our study focused on elucidating the functional significance of observed changes in specific metabolites and integrating all metabolite data into genes and pathways to achieve an overall understanding of signal and metabolic processes after *C. fructicola* inoculation in octoploid strawberries.

Conclusions

In this study, we performed a multi-omics analysis to unveil the resistance against C. *fructicola* in different octoploid strawberries. We identified the core DAMs and DEGs related to *C.fructicola* resistance at different stages after C.*fructicola* infection. The phenylpropanoid pathway related to chloroplasts and starch and sugar metabolism plays an important role in the regulation of *C.fructicola* resistance. Furthermore, The phenylalanine is significantly induced at different stages after *C.fructicola* infection. We have also verified that the core differentially expressed genes, such as chlorophyll-related genes, alpha amylase genes, glycosyl hydrolase (GH) family genes, berberine, peroxidase and catechin biosynthesis gene, are responded to *C.fructicola* infection. Therefore, our study might reveal the multi-level regulatory network by reprogramming the phenylpropanoid biosynthesis related pathways involved in the regulation of *C.fructicola* resistance.

Supplementary Information

The online version contains supplementary material available at https://doi.org/10.1186/s12870-025-06057-0.

Supplementary Material 1

Supplementary Material 2

Supplementary Material 3

Supplementary Material 4

Supplementary Material 5

Acknowledgements
Not applicable.

Author contributions
Xiaohua Zou: Conceptualization, Methodology, Data curation, Formal analysis, Investigation, Validation, Visualization, Writing-original draft. Yun Bai: Investigation, Data curation. Ying Ji: Investigation. Liqing Zhang: Validation. Qinghua Gao: Editing. Xianping Fang: Editing, Manuscript revision, Funding acquisition.

Funding
This work was supported by Shanghai Agricultural Science and Technology Innovation Program, China (Grant No. 2024-02-08-00-12-F00010).

Data availability
All data generated and analyzed during this study are included in this published article and its supplementary information files. The datasets generated and analysed during the current study are available in the Sequence Read Archive (SRA) repository in National Center for Biotechnology Information (NCBI) under the accession number PRJNA1094606.

Declarations

Ethics approval and consent to participate
Not applicable.

Consent for publication
Not applicable.

Competing interests
The authors declare no competing interests.

Received: 25 March 2024 / Accepted: 3 January 2025
Published online: 13 February 2025

References

1. Dubrow GA, Forero DP, Peterson DG. Identification of volatile compounds correlated with consumer acceptability of strawberry preserves: untargeted GC-MS analysis. Food Chem. 2022;1(378):132043.
2. Mao J, Wang Y, Wang B, Li J, Zhang C, Zhang W, Li X, Li J, Zhang J, Li H. High-quality haplotype-resolved genome assembly of cultivated octoploid strawberry. Hortic Res. 2023;10(1):299–310.
3. Wu YM, Chen X, Wang F, Hsiao CY, Yang CY, Lin ST, Wu LH, Chen YK, Liang YS, Lin YH. *Bacillus amyloliquefaciens* strains control strawberry anthracnose through antagonistic activity and plant immune response intensification. Biol Control. 2021;157:104592.
4. Denoyes-Rothan B, Guérin G, Délye C, Smith B, Freeman S. Genetic diversity and pathogenic variability among isolates of *colletotrichum* species from strawberry. Phytopathology. 2003;93(2):219–28.
5. Van HW, Debode J, Heungens K, Maes M, Creemers P. Phenotypic and genetic characterization of *Colletotrichum* isolates from Belgian strawberry fields. Plant Pathol. 2010;59(5):853–61.
6. Xie L, Zhang J-z, Wan Y, Hu D-w. Identification of *Colletotrichum* spp. isolated from strawberry in Zhejiang Province and Shanghai city, China. J Zhejiang Univ Sci B. 2010;11(1):61–70.
7. Ji Y, Li X, Gao QH, Geng C, Duan K. *Colletotrichum* species pathogenic to strawberry: discovery history, global diversity, prevalence in China, and the host range of top two species. Phytopathol Res. 2022;4(1):1–16.
8. Zou X, Guo R, Zhang L, Duan K, Gao Q. Identification of FaNBS-encoding genes responsive to *Colletotrichum fructicola* infection in strawberry (*Fragaria ×ananassa* Duch). Australas Plant Pathol. 2018;47(5):499–510.
9. He C, Duan K, Zhang L, Zhang L, Song L, Yang J, Zou X, Wang Y, Gao Q. Fast quenching the burst of host salicylic acid is common in early strawberry/Colletotrichum fructicola interaction. Phytopathology. 2019;109(4):531–41.
10. Zhang L, Huang X, He C, Zhang QY, Zou X, Duan K, Gao Q. Novel fungal pathogenicity and leaf defense strategies are revealed by simultaneous transcriptome analysis of *colletotrichum fructicola* andstrawberry infected by this fungus. Front Plant Sci. 2018;9:434.
11. Wang F, Zhang F, Chen M, Liu Z, Zhan Z, Fu J, Ma Y. Comparative transcriptomics reveals differential gene expression related to *Colletotrichum gloeosporioides* resistance in the octoploid strawberry. Front Plant Sci. 2017;8(15):779.
12. Fang X, Chai W, Li S, Zhang L, Yu H, Shen J, Xiao W, Liu A, Zhou B, Zhang X. HSP17.4 mediates salicylic acid and jasmonic acid pathways in the regulation of resistance to *Colletotrichum gloeosporioides* in strawberry. Mol Plant Pathol. 2021;22(7):817–28.
13. Zou X-H, Dong C, Liu H-T, Gao Q-H. Genome-wide characterization and expression analysis of WRKY family genes during development and resistance to *Colletotrichum fructicola* in cultivated strawberry (*Fragaria × ananassa* Duch). J Integr Agric. 2022;21(6):1658–72.
14. Aerts N, Mendes MP, Wees SCMV. Multiple levels of crosstalk in hormone networks regulating plant defense. Plant J. 2020;105(2):489–504.
15. Francisco AR, José G, José G, Rosario BP, Antonio MM, Oswaldo T, Berta D, Arroyo FT, Ana AP, Fernando R. Partial activation of SA-and JA-defensive pathways in strawberry upon *Colletotrichum acutatum* interaction. Front Plant Sci. 2016;7(170):1–23.
16. Song XL, Zhang X, Dong QH, Guo B. The establishment of the recipient systems of genetic transformation from 'Benihoppe' strawberry (*Fragaria ×ananassa* Duch). Acta Hort. 2016;3(1049):377–81.
17. Zhang Q, Zhang L, Song LL, Duan K, Li N, Wang Y, Gao Q. The different interactions of *Colletotrichum gloeosporioides* with two strawberry varieties and the involvement of salicylic acid. Hortic Res. 2016;003(001):277–86.
18. Clancy MA, Rosli HG, Chamala S, Barbazuk WB, Civello PM, Folta KM. Validation of reference transcripts in strawberry (*Fragaria* spp). Mol Genetics&Genomics. 2013;288:671–81.
19. Mochizuki Y, Iwasaki Y, Funayama M, Ninomiya S, Ogiwara I. Analysis of a high-yielding strawberry (*Fragaria×ananassa* Duch.) Cultivar 'Benihoppe' with focus on dry matter production and leaf photosynthetic rate. J Japanese Soc Hortic Sci. 2013;82(1):22–9.

20. Chandler CK, Albregts EE, Howard CM, Brecht JK. Sweet Charlie' strawberry. HortScience. 2005;32(6):1132–3.
21. Szklarczyk D, Santos A, Vonmering C, Jensen LJ, Kuhn M. STITCH 5: augmenting protein-chemical interaction networks with tissue and affinity data. Nucleic Acids Res. 2015;44(D1):380–4.
22. Desmedt W, Jonckheere W, Nguyen VH, Ameye M, Zutter ND, Kock KD, Debode J, Leeuwen TV, Audenaert K, Vanholme B, et al. The phenylpropanoid pathway inhibitor piperonylic acid induces broad-spectrum pest and disease resistance in plants. Plant Cell Environ. 2021;44(9):3122–39.
23. Shi J, Yan X, Sun T, Shen Y, Shi Q, Wang W, Bao M, Luo H, Nian F, Ning G. Homeostatic regulation of flavonoid and lignin biosynthesis in phenylpropanoid pathway of transgenic tobacco. Gene. 2022;809(30):146017.
24. Ramaroson M, Helesbeux J, Hamama L, Oge L, Breard D, Huet S, Suel A, Hugueney P, Baltenweck R, Claudel P. Deciphering the role of three specific flavonoids produced by carrot as potential breeding markers for resistance against *Alternaria Dauci*. Acta Hort. 2023;1362:313–20.
25. Bauters L, Stojilkovi B, Gheysen G. Pathogens pulling the strings: effectors manipulating salicylic acid and phenylpropanoid biosynthesis in plants. Mol Plant Pathol. 2021;22(11):1436–48.
26. Ranjan A, Westrick NM, Jain S, Piotrowski JS, Ranjan M, Kessens R, Stiegman L, Grau CR, Conley SP, Smith DL. Resistance against *Sclerotinia sclerotiorum* in soybean involves a reprogramming of the phenylpropanoid pathway and up-regulation of antifungal activity targeting ergosterol biosynthesis. Plant Biotechnol J. 2019;17:1567–81.
27. Tang B, Liu C, Zhang LZ, Zhou X, Wang S, Chen G-L, Liu X-L. Multilayer regulatory landscape during pattern-triggered immunity in rice. Plant Biotechnol J. 2021;19:2629–45.
28. Abbey J, Jose S, Percival D, Jaakola L, Asiedu S. Modulation of defense genes and phenolic compounds in wild blueberry in response to *Botrytis Cinerea* under field conditions. BMC Plant Biol. 2023;23:117.
29. Ranjan A, Westrick NM, Jain S, Piotrowski JS, Ranjan M, Kessens R, Stiegman L, Grau CR, Conley SP, Smith DL. Resistance against Sclerotinia sclerotiorum in soybean involves a reprogramming of the phenylpropanoid pathway and up-regulation of antifungal activity targeting ergosterol biosynthesis. Plant Biotechnol J. 2019;17(8):1567–81.
30. Kumar V, Nadarajan S, Boddupally D, Wang R, Bar E, Davidovich-Rikanati R, Doron-Faigenboim A, Alkan N, Lewinsohn E, Elad Y. Phenylalanine treatment induces tomato resistance to Tuta absoluta via increased accumulation of benzenoid/phenylpropanoid volatiles serving as defense signals. Plant J. 2024;119(1):84.
31. Kim DS, Hwang BK. An important role of the pepper phenylalanine ammonia-lyase gene (PAL1) in salicylic acid-dependent signaling of the defense response to microbial pathogens. J Exp Bot. 2014;65(9):2295–306.
32. Rey J, Nicolas. Piasecka, Anna, Bednarek, Pawel. Secondary metabolites in plant innate immunity: conserved function of divergent chemicals. New Phytol. 2015;206(3):948–64.
33. Piasecka A, Jedrzejczak-Rey N, Paweł Bednarek P. Secondary metabolites in plant innate immunity: conserved function of divergent chemicals. New Phytol. 2015;206:948–64.
34. Huang Y, Xiong Q, Li X, Zhang Y, Gan CF, Peng Z, Wang L, Cui J. Synthesis, characterization and application of emamectin-alkaline lignin conjugate with photolysis resistance and systemic translocation. Int J Biol Macromol. 2023;240:124450.
35. Gupta A, Awasthi P, Sharma N, Parveen S, Vats RP, Singh N, Kumar Y, Goel A, Chandran D. Medicarpin confers powdery mildew resistance in *Medicago truncatula* and activates the salicylic acid signalling pathway. Mol Plant Pathol. 2022;23(7):966–83.
36. Han P, Wei Y, Jiang S, Chen Y, Xu F, Wang H, Shao X. N-Acetyl-D-glucosamine inhibition of hexokinase results in downregulation of the phenylpropanoid metabolic pathway and decreased resistance to brown rot in peach fruit. J Agric Food Chem. 2022;70(12):3917–28.
37. Yang J, Ma L, Jiang W, Yao Y, Pang Y. Comprehensive identification and characterization of abiotic stress and hormone responsive glycosyl hydrolase family 1 genes in Medicago truncatula. Plant Physiol Biochem. 2020;158:21–33.
38. Yang C, Liu R, Pang J, Ren B, Liu J. Poaceae-specific cell wall-derived oligosaccharides activate plant immunity via *OsCERK1* during *Magnaporthe oryzae* infection in rice. Nat Commun. 2021;12(1):1–13.
39. Sivaramakrishnan M, Chandrasekar CVNPB. Multifaceted roles of plant glycosyl hydrolases during pathogen infections: more to discover. Planta. 2024;259(5):1–24.
40. Kang L, Li C, Qin A, Liu Z, Li X, Zeng L, Yu H, Wang Y, Song J, Chen R. Identification and expression analysis of the nucleotidyl transferase protein (NTP) family in soybean (*Glycine max*) under various abiotic stresses. Int J Mol Sci. 2024;25(2):1115.
41. Medina-Puche L, Tan H, Dogra V, Wu M, Lozano-Duran R. A defense pathway linking plasma membrane and chloroplasts and co-opted by pathogens. Cell. 2020;182(5):1109–24.
42. Wu X, Zhou X, Lin T, Zhang Z, Wu X, Zhang Y, Liu Y, Tian Z. Accumulation of dually-targeted StGPT1 in chloroplasts mediated by StRFP1, an E3 ubiquitin ligase, enhances plant immunity. Hortic Res. 2024;8(30):1–34.
43. Attila á, Zoltán N, Gyrgy K, Emese M, Orsolya V. Signals of systemic immunity in plants: progress and open questions. Int J Mol Sci. 2018;19(4):1146.

Publisher's note